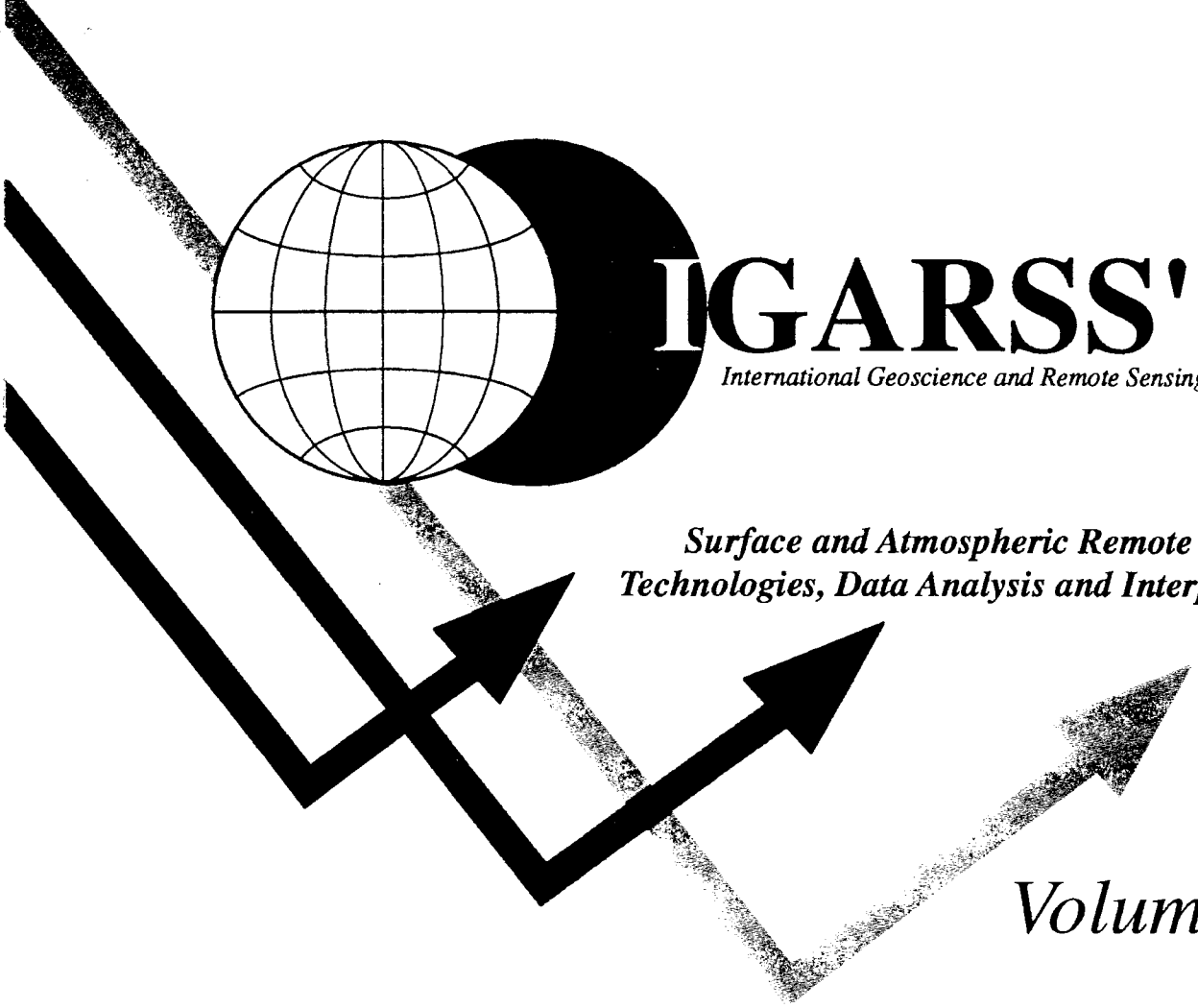

IGARSS'94

International Geoscience and Remote Sensing Symposium

Surface and Atmospheric Remote Sensing: Technologies, Data Analysis and Interpretation

Volume I

California Institute of Technology
Pasadena, California USA
August 8-12, 1994

IEEE

U.R.S.I.

IEEE Catalog Number 94CH3378-7
Library of Congress Number: 93-80348

LIDAR MEASURED REFRACTIVE EFFECTS IN A COASTAL ENVIRONMENT

D.W. Blood, S. McKinley and C. R. Philbrick
Applied Research Laboratory/Penn State University, P.O. Box 30,
State College, PA 16804
(814) 863-8243, Fax (814) 863-8783

R. Paulus and T. Rogers
NCCOSC (Code 543) RDT&E Division
San Diego, CA 92152-7385
(619) 553-1424, FAX (619) 553-1417

Abstract

Atmospheric refractive profiles have been collected in close succession during 1993 at Pt. Mugu during the VOCAR Campaign using Lidar measured water vapor and temperature profiles. The data provides input to propagation analysis models both to interpret the effects on radio paths and for predictive purposes, once the temporal history and character of the prevailing conditions is known. The Lidar derived refractivity and variability is presented for the period of August 26-27th when intense near-ocean ducting caused enhanced radio signal propagation at VHF to UHF.

INTRODUCTION

Lidar measurements of coastal atmospheric refractive environments were made during the 1993 Summer and Fall VOCAR Campaigns, with the Lidar situated at Pt. Mugu, CA. The PSU/LAMP LIDAR (Philbrick, 1994) was used to obtain molecular vibrational Raman scattering at 660 and 607nm (green visible) and at UV, for water vapor profiles. Temperature profiles were obtained by rotational Raman scattering at 528 and 530nm. For each measurement, the Lidar line-ratio measured data are accumulated and used to compute atmospheric refractivity (N, and modified refractivity M) profiles in the lower tropospheric region (0-5000m). The Lidar collected data permits the examination of the temporal variation of refractive index profiles (30 min. time averages used) from a fixed vertical beam in this application. The refractivity range resolution (altitude) cell is obtained from photon counts in 75m cells, adequate sampling for comparisons with refractive profiles from (drifting) balloon-borne radiosonde instruments. The radiosondes were launched both by PSU at the Lidar, and by the nearby Pt. Mugu weather station typically every 4 hours during the VOCAR test periods.

The Lidar derived refractivity profiles are analyzed for refractive layer structures and the EM wave propagation environment. The propagation effects influence systems performance in the Southern California near-coastal atmosphere (SOCAL) and similar world ocean environments (Richter, 1989). During the summer at Pt. Mugu, near-surface humid atmospheric conditions, accompanied by temperature inversion layers, produced periods of persistent surface and near-surface refractive ducts (trapping layers) affecting laterally propagating radio waves.

The effects of the ocean/coastal meteorological conditions on wave propagation were sensed by measuring the signals received from several (existing) VHF and UHF airport ATIS & MCAS, and (installed) VOCAR radio transmitters at the San Clemente Is. NAS. The receiving, monitoring, and recording systems (at Pt. Mugu and San Diego) were all provided by NCCOSC/NRaD (co-author T. Rogers) for use during the VOCAR operations. While the Lidar (and radiosonde) derived refractive measurements are analyzed to specify the propagation environmental conditions, the ocean and coastal radio paths are analyzed for path signal levels and signal amplitude variability. The propagation conditions were modeled through the use of the Navy's IREPS, EREPS and RPO propagation programs.

OBSERVATIONS

Lidar Measurement Capability

Lidar derived profiles permit the examination of the short term (hour-to-hour) variations throughout a day. The refractive layer temporal structure and vertical stratifications, producing the guided-wave mode propagation and multipath mode interference, may be examined in detail. A time sampling of 30 minutes was used in the cases presented. Shorter spaced time sampling of Lidar profiles of 15 minutes or less (not presently analyzed) would provide a further detailed examination of temporal structure.

Basic Measurements of Refractive Index

A series of Lidar refractivity profiles on two consecutive night-to-day periods during August 1993 have been analyzed to examine temporal and vertical structure and variation. Examples of the basic measurements of water vapor (specific humidity, g/kg) and temperature (deg. K) are shown in Figures 1 and 2 respectively, with near-time radiosonde profiles. The resulting refractivity (N), Fig. 3, and modified refractivity (M), Fig. 4 profiles are shown for altitudes of 0-1500m for three 30 min. time accumulation periods. The rapid drop in water vapor with altitude coincides with the temperature inversion (positive lapse rate) profile, Fig. 2, to produce a strong trapping layer to heights of 600m on Aug. 26th., (350m on Aug. 27th.).

Time History - 26, 27 Aug. 93 - Pt. Mugu PSU Lidar

The data series is given in Figures 5 and 6, in terms of 3-D surface plots (refractivity only). Analysis has been performed (Helvey,1994), indicating that the M-profile refractive duct height and temporal history agrees with that derived from longer term radiosonde sampling throughout the same period. The detailed structure reveals sub layers which appear and fade somewhat throughout the time period. The persistent near-surface trapping layer is evident throughout the entire period. This is coincident with the extended-range (enhanced) signal level propagation on the over-ocean and coastal VHF and UHF radio paths.

Application of N-Profiles to Propagation Models

Given the measured refractivity profile(s), analysis of propagation path losses, raytracings and guided-mode wave propagation (parabolic equation) can be exercised through the use of the Navy's IREPS (Hitney,1985), EREPS (Hitney, 1989), and RPO (Radio Physical Optics, Paulus, 1994) propagation models & analysis PC programs. An example of the use of the use of RPO with a single vertical refractivity profile from the Pt. Mugu Lidar is given in Figure 7, showing a leaking waveguide at modal points.

Radio Measurements

The long term (day-to-day) effects show correlation between over all high signal levels and the presence of persistent surface-based ducts as measured with the Lidar. The strongest signal levels on long beyond-the-horizon paths can reach or exceed free space propagation predictions on the 130 km ocean path from San

0-7803-1497-2/94 $4.00

Clemente Is.-to-Point Mugu (at UHF, Fig. 8). The received signal levels differ over the long term by as much as 40dB (conditions ranging from super-refractive to sub-refractive), often with persistence of one-to-two days at levels differing by tens of dB. The frequency separated VHF (143 MHz) and UHF (375 MHz) received signals show level (RSL) variations that are also highly correlated (Figs. 8 & 9), on shorter term time scales of order one hour or less (signals continually sampled each 15 minutes). This suggests that the wave-guide mode effects are governed both by the duct (strength & height) temporal stability and the interfering mode effects set up within the stratified trapping layers. On other over ocean and coastal spatially separated paths, a mixture of correlated and uncorrelated effects are observed, sometimes showing delays relatable to advecting moisture fronts (largely westerly winds) bringing ocean air environments toward the coastal region.

The radio wave raypaths are injected & concentrated into trapping layers at near-grazing incidence angles of +/- 0.2 degrees from the horizontal with antennas heights of a few 10s of meters that are within near-surface super-refractive layers of a few 100m thickness. Rarely are elevated ducts above several hundred meters influential in trapping waves over path distances of tens-to-hundreds of kilometers due to the non-grazing angle of incidence at the layer.

SUMMARY

The Lidar instrument for rapid refractive index profiling provides input for detailed analysis of refractive effects on EM systems. Radiosonde wind measurements, together with available propagation analysis models provide the tools for the analysis. Though not discussed, the signal levels are qualitatively predicted. The limited Lidar data analyzed suggests that the causes of time-varying structure can be further understood with the existing VOCAR data base and further analysis.

REFERENCES

Helvey, R., et. al: "LIDAR and Radiosonde Measurements of Coastal Atmospheric Refraction," Proc. SPIE Conf., Vol. 2222, Orlando FL, March 1994.

Hitney, H.V., J.H. Richter, R.A. Pappert, K.D. Anderson, and G.B. Baumgartner, Jr.: "Tropospheric Radio Propagation Assessment," Proc. IEEE, Vol. 73, No. 2, Feb. 1985, pp. 265-283.

Hitney, H.V: "Engineer's Refractive Effects Prediction System (EREPS)," NATO AGARD Conf. Proc., Operational Aids for Exploiting or Mitigating EM Propagation Effects," AGARD-CP-453, 15-19 May 1989 Symp., Sept. 1989, pp. 6-1 to 6-10.

Paulus, R.A: "The Lorentz Reciprocity Theorem and Range-Dependent Propagation Modeling," IEEE Trans. Ant. & Prop., Vol. 42, No. 2, Feb. 1994, pp. 270-273.

Philbrick, C.R., D.B. Lysak, T.D. Stevens, P.A.T. Haris and Y.-C. Rau: "LIDAR Measurements of Middle and Lower Atmosphere Properties During the LADIMAS Campaign," Proc. 11th. ESA Symp. Eur. Rocket & Balloon Programmes, Montreux, Switzerland, 24-28 May 1993, ESA SP-355, March 1994, pp. 223-228.

Richter, J.H: "Propagation Assessment and Tactical Decision Aids," NATO/AGARD Conf. Proc., Operational Aids for Exploiting or Mitigating EM Propagation Effects," AGARD-CP-453, 15-19 May 1989 Symp., Sept. 1989, pp. 2-1 to 2-8.

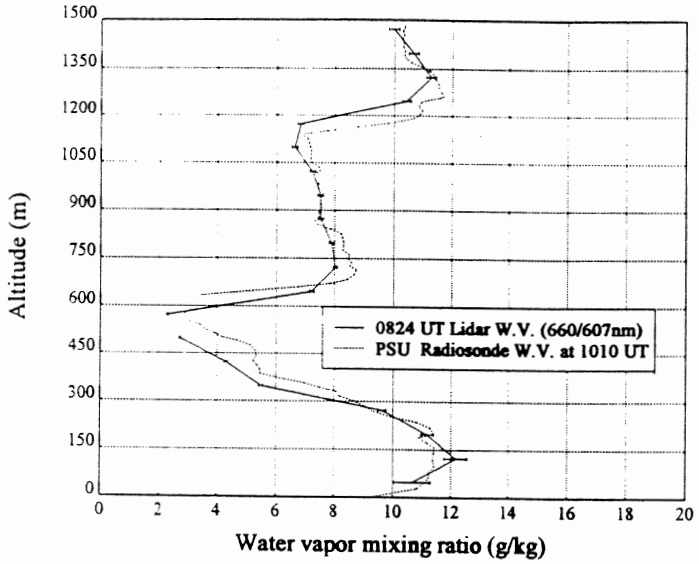

Figure 1.
Lidar water vapor mixing ratio (specific humidity, g/kg), compared with radiosonde profile, 26 August 1993 (std. dev. error bars shown on Lidar)

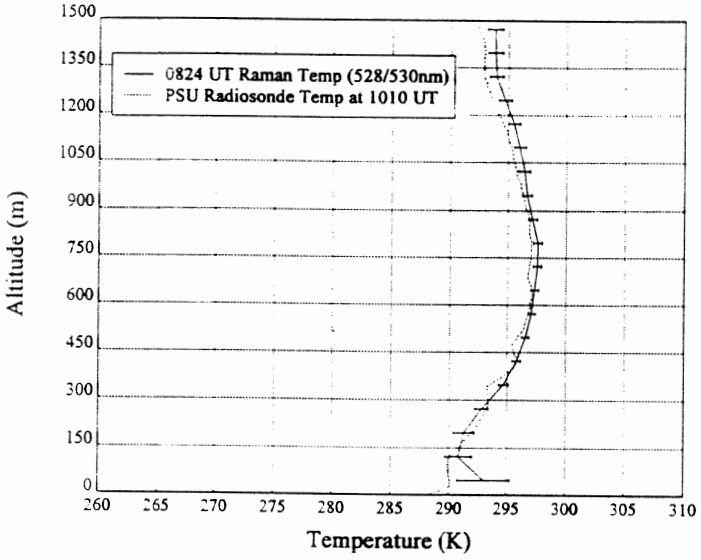

Figure 2.
Lidar & radiosonde temperature profiles, 26 August 1993

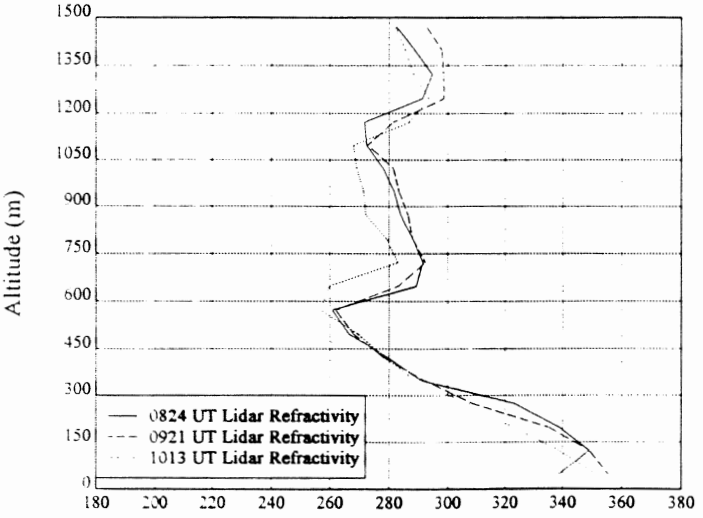

Figure 3.
Refractivity (N) profiles in succession, 26 August 1993

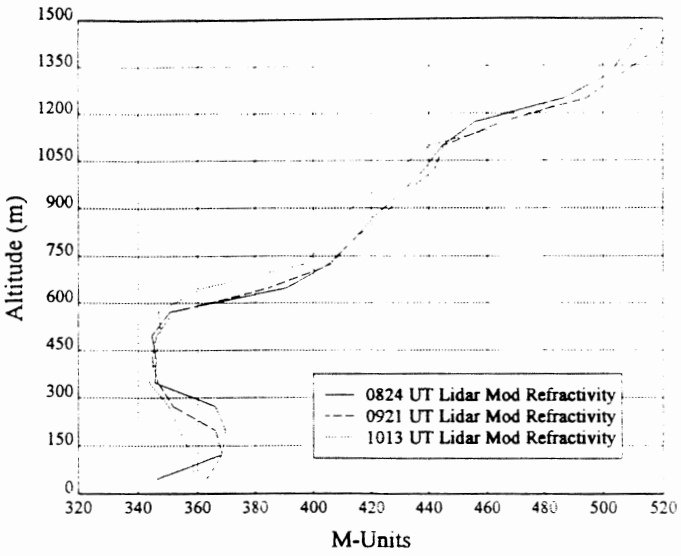

Figure 4.
Modified Refractivity (M) profiles, 26 August 1993

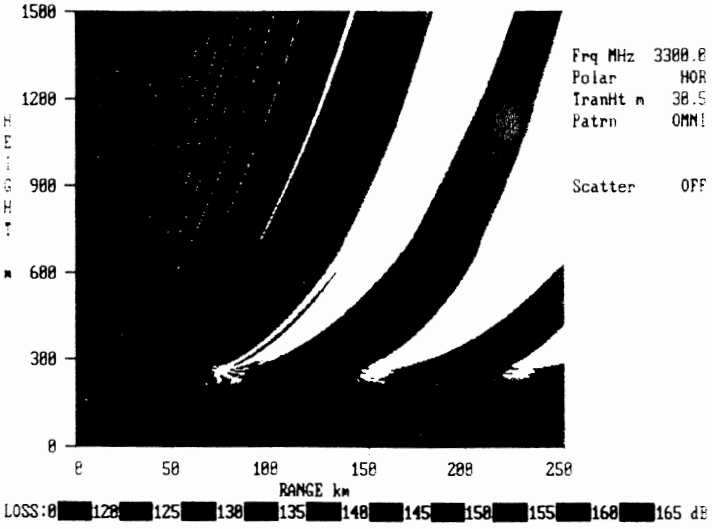

Figure 7.
Coverage plot obtained with RPO and a Pt. Mugu PSU/ARL Lidar refractivity with surface ducting. 08/26/93, 1013 UT.

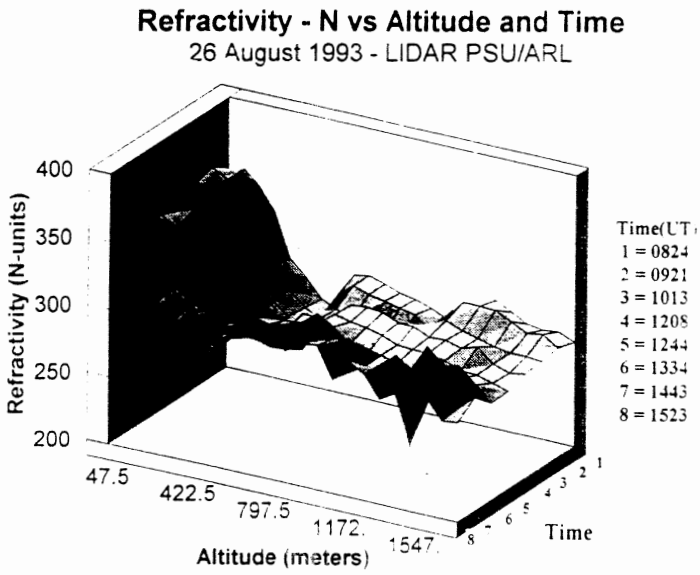

Figure 5.

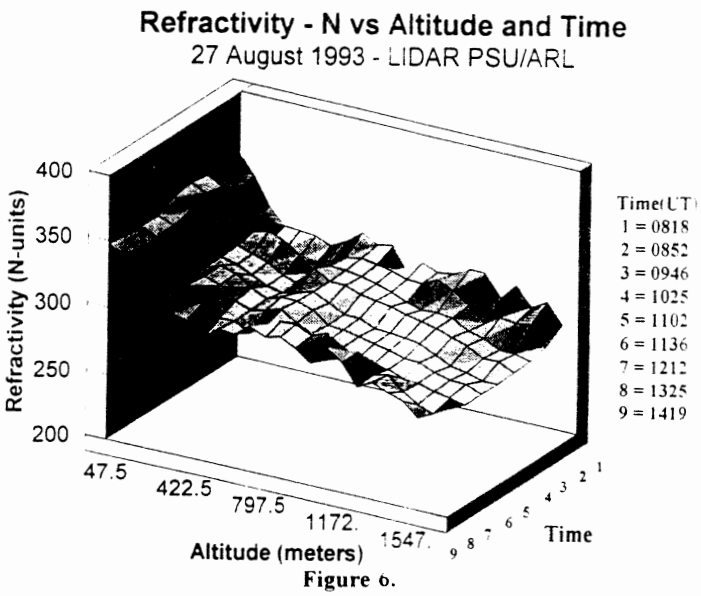

Figure 6.

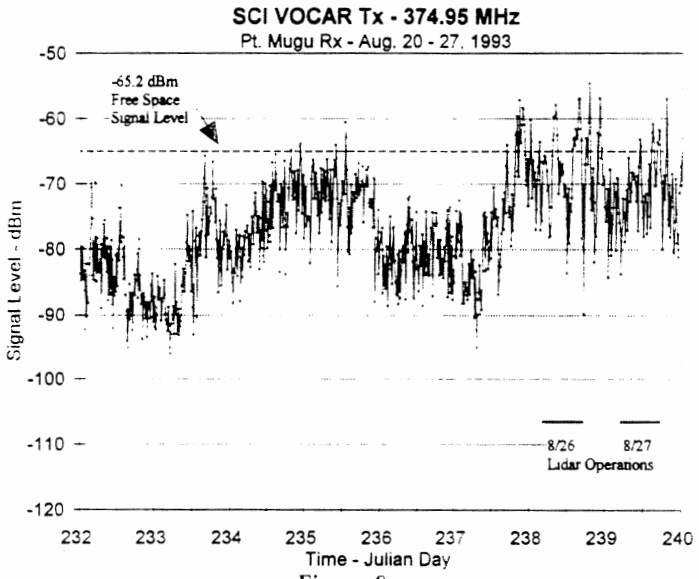

Figure 8.
Received Signal Level (RSL) at UHF - Ocean Path

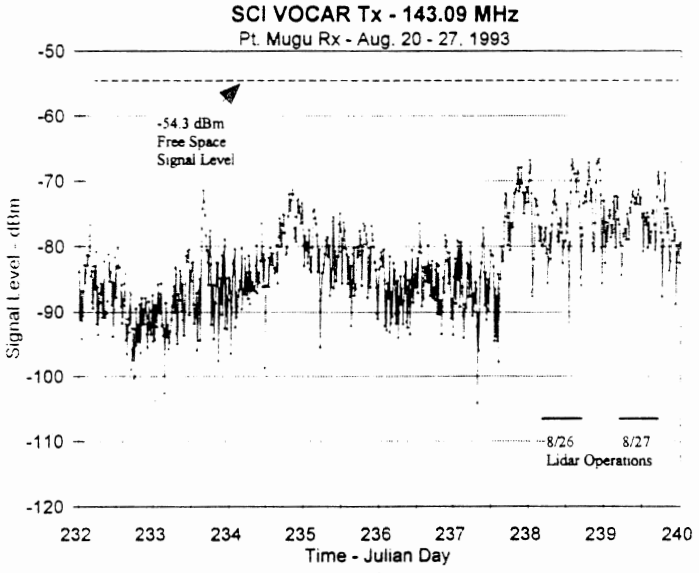

Figure 9.
Received Signal Level at VHF